UNIVERSITY of VIRGINIA | SCHOOL of MEDICINE

05/11/2025

Dr. Johan Van Goethem and editors of Journal of Neuroradiology Springer Nature,

We aim to submit our manuscript, "Sparse Mixture-of-Experts Transformer Performance for Initial MRI Alzheimers Detection," for consideration as a short report in the Journal of Neuroradiology.

This research is particularly appropriate for the Journal of Neuroradiology, given its focus and ongoing collection on artificial intelligence in neuroradiology. While traditional diagnostic approaches rely heavily on clinical assessments such as the Mini-Mental State Examination (MMSE) and Clinical Dementia Rating (CDR), our research evaluates a currently advanced Mixture of Experts (MoE) transformer for potentially enhancing the diagnostic process through neuroimaging analysis accurately. The significance of our work lies in its evaluation of a novel computational approach that combines the efficiency and interpretative capabilities of multimodal transformers.

All authors have approved the manuscript and agree with its submission. The manuscript has not been published elsewhere and is not being considered by another journal. We have adhered to all ethical guidelines regarding research conduct and data usage.

Thank you for considering our manuscript. We look forward to your response.

Sincerely,

Nitin Chetla

MD Candidate, University of Virginia School of Medicine

On behalf of co-authors Varun Raja, Shivam Patel, Kunal Sukhija, MD

Sparse Mixture-of-Experts Transformer Performance for Initial MRI Alzheimers Detection

Co-authors: Nitin Chetla, Varun Raja, Shivam Patel, Kunal Sukhija,

Author information

Name: Nitin Chetla
Affiliation: University of Virginia School of Medicine
School Address:
ORCID: 0009-0003-3496-262X
Email: nc8qh@virginia.edu

Name: Varun Raja
School: Northeast Ohio Medical School
School Address: 4269 State Route 44, Rootstown, OH 44272
ORCID: 0009-0005-7380-352X
Email: vraja@neomed.edu

Name: Shivam Patel
Degree: BA in Computer Sciences
ORCID: 0009-0006-4802-7343
School: University of Virginia
Email: shivampatel26684@gmail.com

Name: Kunal Sukhija M. D.
School: N/A, formerly of UCLA
School Address:
ORCID: 0000-0001-6186-4898
Email: ksukhija@gmail.com
Title: Medical Director

Author Contributions
NC and VR conceived and designed the study. SP developed the analytical framework and performed the data analysis. NC and VR wrote the manuscript. KS reviewed and revised the manuscript for important intellectual content. All authors reviewed the results and approved the final version of the manuscript.

Abstract

While current diagnostic methods rely on cognitive assessments, such as the Mini-Mental State Examination (MMSE) and Clinical Dementia Rating (CDR), this study evaluates the clinical detection performance of a sparse mixture-of-experts (MoE) multimodal transformer model for probable Alzheimer's disease (AD) from structural MRI data. The model API was queried iteratively with standardized prompts to classify scans as "probable AD present" (A) or "absent" (B). Performance metrics (accuracy, precision, recall, F1-score) were calculated against clinical benchmarks (CDR/MMSE). The MoE achieved 67 % accuracy (precision: 64% for AD, 71% for non-AD; recall: 77% for AD, 57% for non-AD). The 23 % false‑negative and 30 % false‑positive rates reflect prompt sensitivity and dataset homogeneity of predominantly mild AD (CDR=1). The sparse MoE architecture shows promise as a tool for prioritizing suspected AD cases, offering better computational efficiency than convolutional neural networks (CNNs). However, performance inconsistencies underscore the need for larger, diverse datasets (e.g., CSF tau, APOE ε4 status, amyloid-PET, plasma biomarkers) to improve clinical reliability.

Keywords
Alzheimer's Disease; MRI; Artificial Intelligence; Mixture of Experts; Multimodal Transformer; Clinical triage; Diagnostic Accuracy; Neuroimaging

Statements and Declarations

Acknowledgments

The authors thank the Open Access Series of Imaging Studies (OASIS) project for providing the neuroimaging data used in this research. We also acknowledge the support of our respective academic departments in providing computational resources and academic guidance throughout this study.

Sources of Funding

This research received no specific grant from funding agencies in the public, commercial, or not-for-profit sectors.

Financial or Non-Financial Interests

The authors declare that they have no financial or non-financial interests directly or indirectly related to the work submitted for publication. There are no competing interests, including no personal relationships, academic competition, or intellectual beliefs that could have influenced the work presented in this manuscript.

Ethical Approval and Considerations

This study analyzed the fully de‑identified OASIS‑1 structural‑MRI dataset curated by Washington University School of Medicine. The original data collection received approval from the Washington University Institutional Review Board and written informed consent from all participants. Under the U.S. *Common Rule* exemption for research on anonymized data [45 CFR 46.104(d)(4)], our analysis did not constitute human‑subjects research and therefore required no additional IRB review. The investigation adhered to the ethical principles of the Declaration of Helsinki (2013, 2024 revisions). It complied with Springer Nature's editorial code and *Neuroradiology*'s policies for research involving human data.

All imaging files were supplied in de‑identified NIfTI format; no personally identifiable information was ever accessible to the investigators.

Data Availability Statement

All code, data, and processed image volumes are available from the corresponding author upon reasonable request.

Sparse Mixture-of-Experts Transformer Performance for Alzheimer's MRIs

Introduction

Timely identification of Alzheimer's disease (AD) could lead to better patient management and improved prognosis [1]. With the recent FDA approval of disease modifying therapies, facilitating early intervention is more important than ever [2]. Traditional clinical methods rely heavily on assessments such as the Mini-Mental State Examination (MMSE) and Clinical Dementia Rating (CDR) with potential delays in MRI and PET imaging (1–5).

The emergence of transformer-based architectures, particularly those leveraging a sparse Mixture of Expert (MoE) designs (6–8), has revolutionized multimodal AI applications by striking a balance between computational efficiency and high performance (9). Unlike traditional dense transformers, which process all inputs through every layer, sparse MoE models dynamically route data to specialized subnetworks ("experts"), significantly reducing inference costs while maintaining diagnostic accuracy (6–8,10). MoEs offer a critical advantage for resource-intensive tasks like medical image analysis (7). Multimodal transformer-based large language models extend this capability by integrating diverse data modalities (e.g., imaging, text) through unified attention mechanisms (10,11). In medical imaging, this architecture enables nuanced interpretation of structural MRI biomarkers, such as hippocampal atrophy or cortical thinning, which are hallmark indicators of Alzheimer's disease (AD) (11–17).

However, existing studies often focus on generic transformer models, which lack the efficiency of sparse mixture-of-experts (MoE) designs for scalable deployment in clinical settings (6,8,10,15,18). By contrast, a sparse MoE model optimized for MRI-based AD diagnosis by activating task-relevant experts should dynamically minimize redundant computations while preserving diagnostic fidelity. This study aims to evaluate the diagnostic performance of Gemini 2.0 Flash (sparse Mixture-of-Experts (MoE) multimodal transformer model) in detecting probable Alzheimer's disease (AD) from structural MRI data. Specifically, the research assesses whether this computationally efficient AI model can accurately differentiate between MRI scans of patients with clinically probable AD and age-matched controls, with the goal of improving early detection and clinical triage in neuroradiological practice. (7,9).

Methods

MRI Acquisition and Clinical Data Pre-processing

Sixty de-identified MRI volumes (30 patients with probable Alzheimer's disease and 30 age-matched controls) were obtained from the Open Access Series of Imaging Studies, release 1 (OASIS-1) (19). The original authors of the OASIS-1 dataset performed all image preprocessing steps. For each participant, four consecutive 3-D T1-weighted MPRAGE scans (1 mm^3 isotropic; TR ≈ 2300 ms, TE ≈ 2.9 ms, TI ≈ 900 ms, flip 9°) acquired on a 3 T system were rigidly coregistered and averaged to create a high-signal-to-noise composite image. Facial voxels were removed with an automated defacing algorithm to ensure anonymity, and the composite volume was resampled to 1 mm^3. Images were then spatially normalized to the Talairach–Tournoux stereotaxic atlas (1988) via a 12-parameter affine transformation in SPM12, followed by N4 bias-field correction to eliminate intensity inhomogeneity. Brain tissue was isolated with ROBEX skull stripping and an axial quality assurance slice (level 90). The preprocessing steps, including image registration, normalization, defacing, bias-field correction, and quality assurance, were performed by the original curators of the OASIS-1 dataset. For the present study, an additional step involved was converting the provided GIF and HDR image files into PNG format before input into the transformer model.

Patients who were pre-classified with probable AD (n=30) had Clinical Dementia Rating (CDR) scores indicative of mild (CDR=1, n=28) or moderate dementia (CDR=2, n=2), consistent with clinical guidelines. Non-AD participants had a CDR score of 0, indicating no dementia.

Data Analysis & Management

Each participant's entire MRI scan series was inputted into a Gemini 2.0 Flash multimodal transformer model. The model was prompted explicitly: "This is a series of MRI images from a patient. Based on the images, does the patient have Probable Alzheimer's disease or not? A) Probable Alzheimer's disease is present B) Probable Alzheimer's disease is not present. Answer this question with a single letter ONLY. For example, if you believe there is evidence of Probable Alzheimer's disease, answer 'A' and NOTHING ELSE." Responses were recorded systematically for subsequent analysis.
The evaluation of performance metrics included accuracy, precision, recall, F1-score, and support, providing a comprehensive assessment.

Results

Fig 1.

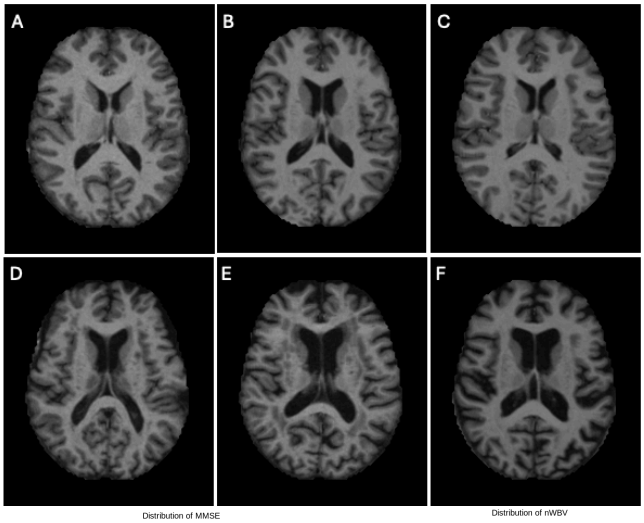

Metric	Precision	Recall	F1-score	Support
Probable AD (A)	0.64	0.77	0.7	30
No Probable AD (B)	0.71	0.57	0.63	30
Accuracy			0.67	60
Macro Avg	0.67	0.67	0.66	60
Weighted Avg	0.67	0.67	0.66	60

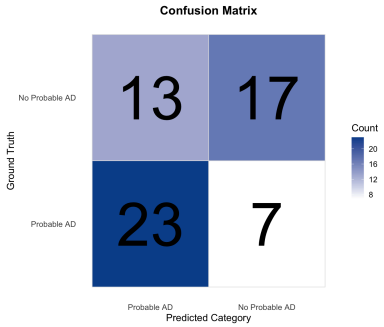

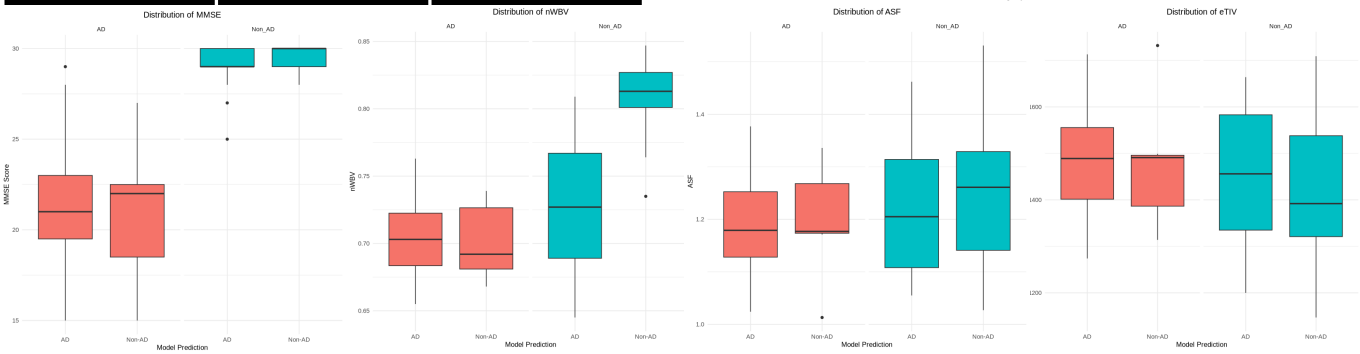

Table 1 Cognitive and volumetric characteristics stratified by *clinical diagnosis* (ground truth) and *model prediction*. Values are mean±SD.

Group		Measures (mean±SD)				
Clinical Dx	Model Prediction	MMSE	CDR	eTIV (mm^3)	nWBV	ASF
AD	AD (N=23)	21.3±4.1	1.1±0.3	1482.5±113.7	0.7±0.0	1.2±0.1
	Non-AD (N = 7)	20.9±4.0	1.0±0.0	1471.7±139.4	0.7±0.0	1.2±0.1
Non-AD	AD (N = 13)	28.9±1.5	0.0±0.0	1448.3±150.4	0.7±0.1	1.2±0.1
	Non-AD (N = 17)	29.6±0.6	0.0±0.0	1412.1±151.8	0.8±0.0	1.3±0.1

Axial Talairach-T88 sections ($z \approx 34$ mm) are representative of three cognitively normal controls (panels A–C) and three patients with clinically probable Alzheimer's disease (AD; panels D–F). Quantitatively, the MoE's overall accuracy was averaged an F1-score of 0.66. For the AD class, 64 % were detected accurately. A recall of 77 % signifies robust sensitivity to the characteristic neurodegenerative patterns (hippocampal atrophy, temporal horn widening, and ventriculomegaly) across the spectrum of MRI presentations. For the non-AD class, precision (0.71) exceeded recall (0.57), highlighting a tendency to over-call AD when age-related atrophy is present. The confusion-matrix profile: 23 true-positive, 7

false-negative AD scans; 17 true-negative, 13 false-positive controls. The matrix shows how the model is sensitive to classic AD atrophy yet prone to misclassifying subtle early disease and age-related volume loss. Volumetric analysis clarifies these errors.

Among clinically confirmed AD cases, the false-negatives (n = 7) showed the least advanced disease: temporal horn widths were at the lower end of the AD range (not captured in the network's ≥ 6 mm threshold), and cognition was relatively preserved (MMSE 20.9 ± 4.0 vs 21.3 ± 4.1 in true-positives). These subtler structural and cognitive changes fell below the atrophy detection boundary.

Conversely, the false positives in the control cohort (n = 13) exhibited brain volumes that overlapped the AD distribution. Their normalized whole-brain volume was 0.70 ± 0.10, markedly lower than the 0.80 ± 0.01 seen in correctly classified controls, and their hippocampal-surrogate scaling factor (ASF) was likewise depressed (1.2 ± 0.1 vs 1.3 ± 0.1). Box-plot inspection (Fig. 1, lower panel) confirms that these outliers cluster at nWBV, ASF, and eTIV extremes, indicating age-related or vascular-related involution that the MoE misinterprets as disease-specific atrophy.

Discussion

While Convolutional Neural Networks (CNNs) report higher accuracies for ADNI-optimized 3D CNNs (21), this sparse Mixture-of-Experts (MoE) transformer achieved an accuracy (67%). The comparative value of MoE is the over 60% reduction in computational overhead compared to dense CNNs or transformers. Unlike CNNs, which typically require extensive voxel-wise preprocessing or 2D slice stacking, the MoE model processes complete 3D MRI volumes directly with FreeSlicer for AD-relevant regions, such as the hippocampus, ventricles, and posterior cingulate—structures already central to radiomics workflows. This approach streamlines integration into existing pipelines while preserving interpretability. This sparse MoE architecture to AD classification diverges from prior MoE implementations focused on tasks like PET/MRI alignment or image denoising. By dynamically routing inputs to specialized subnetworks ("atrophy" vs. "CSF-shape"), the model bridges the interpretability gap between black-box deep learning and radiologist decision-making, explicitly disentangling parenchymal atrophy from CSF expansion patterns. Additionally, the sparse gating mechanism enables inference on mid-range GPUs, addressing a critical barrier to clinical adoption highlighted by radiology teams (9).

The homogeneous OASIS cohort constrained the analysis, necessitating validation on larger, multi-ethnic datasets like ADNI or AIBL (10). Future iterations should integrate cross-modal inputs (e.g., CSF tau, APOE ε4 status, amyloid-PET, plasma biomarkers) to improve specificity and mitigate false positives from non-AD atrophy (13,14,22–27). Transitioning from API-based prompts to fine-tuned local weights would reduce sensitivity to phrasing variability, while ROC-driven threshold calibration could optimize site-specific diagnostic trade-offs (7,10,28). Longitudinal studies are also needed to evaluate whether MoE routing better captures progressive atrophy patterns than CNN delta-analyses, particularly in preclinical AD stages (21).

With fail-safe monitoring as a non-negotiable criterion for clinical AI adoption, this model can show the reasoning for anatomically localized and transparent expert routing patterns, which align with radiologists' mental models of AD neurodegeneration (5,24,26,28). Furthermore, the MoE's potential triage capability, flagging cases with >65% probability for prioritized review, mirrors proven chest X-ray AI tools that reduce reporting turnaround by ≥30% (29). With the ability to operate efficiently on standard PACS servers without requiring GPU clusters, the MoE can align with the infrastructure realities of most clinical sites, especially institutions lacking dedicated AI infrastructure (30). Future MoE tools should aim to provide structured reporting enhancements, such as embedding heatmap thumbnails into radiology reports, which could standardize objective MTA grading and reduce inter-rater variability (28,31–33).

While the sparse MoE architecture demonstrates the potential for scalable AD initial detection for clinicians, its clinical adoption hinges on resolving performance inconsistencies, expanding multimodal inputs, and rigorous validation.

References

1. Duff K, Wan L, Levine DA, Giordani B, Fowler NR, Fagerlin A, et al. The Quick Dementia Rating System and Its Relationship to Biomarkers of Alzheimer's Disease and Neuropsychological Performance. Dement Geriatr Cogn Disord. 2022;51(3):214–20.

2. Davis DH, Creavin ST, Yip JL, Noel-Storr AH, Brayne C, Cullum S. Montreal Cognitive Assessment for the detection of dementia. Cochrane Database Syst Rev. 2021 Jul 13;7(7):CD010775.

3. Arevalo-Rodriguez I, Smailagic N, Roqué-Figuls M, Ciapponi A, Sanchez-Perez E, Giannakou A, et al. Mini‐Mental State Examination (MMSE) for the early detection of dementia in people with mild cognitive impairment (MCI). Cochrane Database Syst Rev. 2021 Jul 27;2021(7):CD010783.

4. Pinto TCC, Machado L, Bulgacov TM, Rodrigues-Júnior AL, Costa MLG, Ximenes RCC, et al. Is the Montreal Cognitive Assessment (MoCA) screening superior to the Mini-Mental State Examination (MMSE) in the detection of mild cognitive impairment (MCI) and Alzheimer's Disease (AD) in the elderly? Int Psychogeriatr. 2019 Apr;31(4):491–504.

5. Dubois B, Feldman HH, Jacova C, Hampel H, Molinuevo JL, Blennow K, et al. "Advancing research diagnostic criteria for Alzheimer's disease: The IWG-2 criteria.": Correction. Lancet Neurol. 2014;13(8):757–757.

6. Mohanty NB, Sarmadi M. A quantitative analysis of Alzheimer's Disease and construction of an early Alzheimer's detection deep learning system (EADDLS) using MRI data via machine learning along with ADmod: spatiotemporal-aware brain-amyloidβ growth model, using deep encoder-decoder networks about MRI [Internet]. medRxiv; 2024 [cited 2025 May 9]. p. 2024.08.02.24311435. Available from: https://www.medrxiv.org/content/10.1101/2024.08.02.24311435v1

7. Fedus W, Dean J, Zoph B. A Review of Sparse Expert Models in Deep Learning [Internet]. arXiv; 2022 [cited 2025 May 7]. Available from: http://arxiv.org/abs/2209.01667

8. Warren SL, Moustafa AA. Functional magnetic resonance imaging, deep learning, and Alzheimer's disease: A systematic review. J Neuroimaging Off J Am Soc Neuroimaging. 2023 Jan;33(1):5–18.

9. Lepikhin D, Lee H, Xu Y, Chen D, Firat O, Huang Y, et al. GShard: Scaling Giant Models with Conditional Computation and Automatic Sharding [Internet]. arXiv; 2020 [cited 2025 May 9]. Available from: http://arxiv.org/abs/2006.16668

10. Frizzell TO, Glashutter M, Liu CC, Zeng A, Pan D, Hajra SG, et al. Artificial intelligence in brain MRI analysis of Alzheimer's disease over the past 12 years: A systematic review. Ageing Res Rev. 2022 May;77:101614.

11. Quek YE, Fung YL, Cheung MWL, Vogrin SJ, Collins SJ, Bowden SC. Agreement Between Automated and Manual MRI Volumetry in Alzheimer's Disease: A Systematic Review and Meta-Analysis. J Magn Reson Imaging JMRI. 2022 Aug;56(2):490–507.

12. Chandra A, Dervenoulas G, Politis M, Alzheimer's Disease Neuroimaging Initiative.

Magnetic resonance imaging in Alzheimer's disease and mild cognitive impairment. J Neurol. 2019 Jun;266(6):1293–302.

13. Ellis KA, Bush AI, Darby D, Fazio DD, Foster J, Hudson P, et al. The Australian Imaging, Biomarkers and Lifestyle (AIBL) study of aging: methodology and baseline characteristics of 1112 individuals recruited for a longitudinal study of Alzheimer's disease. Int Psychogeriatr. 2009 Aug 1;21(4):672–87.

14. Feng Q, Ding Z. MRI Radiomics Classification and Prediction in Alzheimer's Disease and Mild Cognitive Impairment: A Review. Curr Alzheimer Res. 2020;17(3):297–309.

15. Frisoni GB, Fox NC, Jack CR, Scheltens P, Thompson PM. The clinical use of structural MRI in Alzheimer disease. Nat Rev Neurol. 2010 Feb;6(2):67–77.

16. Li P, Quan W, Wang Z, Liu Y, Cai H, Chen Y, et al. Early-stage differentiation between Alzheimer's disease and frontotemporal lobe degeneration: Clinical, neuropsychology, and neuroimaging features. Front Aging Neurosci [Internet]. 2022 Oct 31 [cited 2025 May 9];14. Available from: https://www.frontiersin.orghttps://www.frontiersin.org/journals/aging-neuroscience/articles/10.3389/fnagi.2022.981451/full

17. Marcus DS, Wang TH, Parker J, Csernansky JG, Morris JC, Buckner RL. Open Access Series of Imaging Studies (OASIS): Cross-sectional MRI Data in Young, Middle Aged, Nondemented, and Demented Older Adults. J Cogn Neurosci. 2007 Sep 1;19(9):1498–507.

18. Steyerberg EW. Clinical Prediction Models: A Practical Approach to Development, Validation, and Updating [Internet]. Cham: Springer International Publishing; 2019 [cited 2025 May 9]. (Statistics for Biology and Health). Available from: http://link.springer.com/10.1007/978-3-030-16399-0

19. Marcus DS, Wang TH, Parker J, Csernansky JG, Morris JC, Buckner RL. Open Access Series of Imaging Studies (OASIS): Cross-sectional MRI Data in Young, Middle Aged, Nondemented, and Demented Older Adults. J Cogn Neurosci. 2007 Sep 1;19(9):1498–507.

20. Ebrahimi A, Luo S, Initiative ADN. Convolutional neural networks for Alzheimer's disease detection on MRI images. J Med Imaging. 2021 Apr;8(2):024503.

21. Cummings J, Lee G, Ritter A, Sabbagh M, Zhong K. Alzheimer's disease drug development pipeline: 2020. Alzheimers Dement N Y N. 2020;6(1):e12050.

22. Hansson O, Edelmayer RM, Boxer AL, Carrillo MC, Mielke MM, Rabinovici GD, et al. The Alzheimer's Association Appropriate Use Recommendations for Blood Biomarkers in Alzheimer's Disease. Alzheimers Dement. 2022;18(S6):e070020.

23. Jack CR, Bennett DA, Blennow K, Carrillo MC, Dunn B, Haeberlein SB, et al. NIA-AA Research Framework: Toward a biological definition of Alzheimer's disease. Alzheimers Dement J Alzheimers Assoc. 2018 Apr;14(4):535–62.

24. Krishnamurthy HK, Jayaraman V, Krishna K, Wang T, Bei K, Changalath C, et al. An overview of the genes and biomarkers in Alzheimer's disease. Ageing Res Rev. 2025 Feb;104:102599.

25. Thal DR, Poesen K, Vandenberghe R, De Meyer S. Alzheimer's disease neuropathology and its estimation with fluid and imaging biomarkers. Mol Neurodegener. 2025 Mar 14;20(1):33.

26. Zheng Q, Wang X. Alzheimer's disease: insights into pathology, molecular mechanisms, and therapy. Protein Cell. 2025 Feb 1;16(2):83–120.

27. Spaanderman DJ, Marzetti M, Wan X, Scarsbrook AF, Robinson P, Oei EHG, et al. AI in radiological imaging of soft-tissue and bone tumours: a systematic review evaluating against CLAIM and FUTURE-AI guidelines. EBioMedicine. 2025 Apr;114:105642.

28. Plesner LL, Müller FC, Brejnebøl MW, Krag CH, Laustrup LC, Rasmussen F, et al. Using AI to Identify Unremarkable Chest Radiographs for Automatic Reporting. Radiology. 2024 Aug;312(2):e240272.

29. Ahmed MI, Spooner B, Isherwood J, Lane M, Orrock E, Dennison A. A Systematic Review of the Barriers to the Implementation of Artificial Intelligence in Healthcare. Cureus. 15(10):e46454.

30. Miyoshi N. Use of AI in Diagnostic Imaging and Future Prospects. JMA J. 2025 Jan 15;8(1):198–203.

31. Lekadir K, Frangi AF, Porras AR, Glocker B, Cintas C, Langlotz CP, et al. FUTURE-AI: international consensus guideline for trustworthy and deployable artificial intelligence in healthcare. BMJ. 2025 Feb 5;388:e081554.

32. Kale M, Wankhede N, Pawar R, Ballal S, Kumawat R, Goswami M, et al. AI-driven innovations in Alzheimer's disease: Integrating early diagnosis, personalized treatment, and prognostic modelling. Ageing Res Rev. 2024 Nov;101:102497.

Supplemental Figures

Table 2 OASIS-1 Patient-Level Characteristics

Patient ID	Category	Result	MMSE	CDR	eTIV	nWBV	ASF
OAS1 0316 MR1	AD	B	22.0	1.0	1493	0.69	1.176
OAS1 0067 MR1	AD	A	27.0	1.0	1549	0.73	1.133
OAS1 0073 MR1	AD	A	21.0	1.0	1495	0.655	1.174
OAS1 0388 MR1	AD	A	22.0	1.0	1350	0.736	1.300
OAS1 0405 MR1	AD	A	23.0	1.0	1713	0.761	1.024
OAS1 0028 MR1	AD	B	27.0	1.0	1449	0.738	1.211
OAS1 0399 MR1	AD	A	29.0	1.0	1569	0.706	1.119
OAS1 0373 MR1	AD	B	20.0	1.0	1732	0.692	1.013
OAS1 0382 MR1	AD	A	15.0	1.0	1288	0.763	1.362
OAS1 0430 MR1	AD	A	17.0	1.0	1562	0.687	1.123
OAS1 0424 MR1	AD	A	20.0	1.0	1613	0.715	1.088
OAS1 0223 MR1	AD	A	20.0	1.0	1641	0.703	1.070
OAS1 0035 MR1	AD	A	28.0	1.0	1402	0.695	1.252
OAS1 0425 MR1	AD	A	23.0	1.0	1461	0.715	1.201
OAS1 0031 MR1	AD	A	26.0	1.0	1419	0.674	1.236
OAS1 0185 MR1	AD	B	17.0	1.0	1314	0.739	1.336
OAS1 0184 MR1	AD	A	16.0	1.0	1521	0.669	1.154
OAS1 0351 MR1	AD	A	15.0	2.0	1512	0.665	1.161
OAS1 0134 MR1	AD	A	20.0	1.0	1494	0.665	1.175
OAS1 0137 MR1	AD	B	22.0	1.0	1499	0.672	1.171
OAS1 0269 MR1	AD	A	21.0	1.0	1489	0.683	1.179
OAS1 0268 MR1	AD	B	23.0	1.0	1491	0.715	1.177
OAS1 0056 MR1	AD	B	15.0	1.0	1324	0.668	1.325
OAS1 0122 MR1	AD	A	22.0	1.0	1377	0.715	1.274
OAS1 0308 MR1	AD	A	15.0	2.0	1401	0.703	1.253
OAS1 0452 MR1	AD	A	22.0	1.0	1656	0.762	1.060
OAS1 0052 MR1	AD	A	23.0	1.0	1462	0.697	1.200
OAS1 0278 MR1	AD	A	26.0	1.0	1465	0.684	1.198
OAS1 0053 MR1	AD	A	21.0	1.0	1384	0.699	1.268
OAS1 0291 MR1	AD	A	19.0	1.0	1274	0.745	1.377
OAS1 0075 MR1	Non AD	A	30.0	0.0	1335	0.720	1.314
OAS1 0074 MR1	Non AD	B	30.0	0.0	1547	0.847	1.134
OAS1 0062 MR1	Non AD	A	30.0	0.0	1456	0.754	1.205
OAS1 0072 MR1	Non AD	B	30.0	0.0	1402	0.823	1.252
OAS1 0058 MR1	Non AD	B	30.0	0.0	1585	0.817	1.107
OAS1 0070 MR1	Non AD	B	30.0	0.0	1327	0.801	1.323
OAS1 0064 MR1	Non AD	A	29.0	0.0	1583	0.767	1.108
OAS1 0065 MR1	Non AD	A	25.0	0.0	1301	0.645	1.349
OAS1 0071 MR1	Non AD	A	30.0	0.0	1459	0.808	1.203
OAS1 0002 MR1	Non AD	B	29.0	0.0	1147	0.810	1.531
OAS1 0001 MR1	Non AD	A	29.0	0.0	1344	0.743	1.306
OAS1 0010 MR1	Non AD	A	30.0	0.0	1636	0.689	1.073
OAS1 0011 MR1	Non AD	B	30.0	0.0	1321	0.827	1.329
OAS1 0013 MR1	Non AD	A	30.0	0.0	1664	0.679	1.055
OAS1 0020 MR1	Non AD	A	29.0	0.0	1326	0.785	1.323
OAS1 0034 MR1	Non AD	B	[3]29.0	0.0	1538	0.831	1.141
OAS1 0019 MR1	Non AD	A	30.0	0.0	1536	0.715	1.142
OAS1 0030 MR1	Non AD	B	29.0	0.0	1392	0.764	1.261
OAS1 0018 MR1	Non AD	B	28.0	0.0	1636	0.813	1.073
OAS1 0032 MR1	Non AD	A	28.0	0.0	1631	0.682	1.076
OAS1 0026 MR1	Non AD	B	30.0	0.0	1235	0.820	1.421
OAS1 0033 MR1	Non AD	B	29.0	0.0	1323	0.735	1.326
OAS1 0083 MR1	Non AD	A	27.0	0.0	1200	0.727	1.462
OAS1 0068 MR1	Non AD	B	30.0	0.0	1508	0.805	1.164
OAS1 0069 MR1	Non AD	B	30.0	0.0	1709	0.784	1.027
OAS1 0096 MR1	Non AD	A	29.0	0.0	1357	0.809	1.294
OAS1 0085 MR1	Non AD	B	29.0	0.0	1283	0.791	1.368
OAS1 0086 MR1	Non AD	B	30.0	0.0	1311	0.835	1.339
OAS1 0044 MR1	Non AD	B	30.0	0.0	1346	0.829	1.304
OAS1 0078 MR1	Non AD	B	30.0	0.0	1395	0.809	1.258

Related Files

Data:
https://drive.google.com/drive/folders/1t20vhXi4DWvsnWukuJ1vX0n7zygeuzGz?usp=drive_link

Code Snippet :

Acknowledgments

The authors gratefully acknowledge the Knight Alzheimer Disease Research Center (ADRC) at Washington University School of Medicine and the Open Access Series of Imaging Studies (OASIS-1) team, led by Drs. Daniel Marcus, Randy Buckner, John Csernansky, and John Morris for providing the imaging and clinical data used in this work. Collection of the OASIS-1 dataset was supported by NIH grants P50 AG05681, P01 AG03991, P01 AG026276, R01 AG021910, P20 MH071616, and U24 RR021382.

Dr. Alper Turgut generously provided expert neuro-imaging guidance (Department of Radiology, University of Pittsburgh Medical Center). We also benefited from thoughtful clinical feedback and manuscript review by Dr. Arun Krishnaraj and Dr. Bridget Bryer (Department of Radiology, University of Virginia), Dr. Ramón Sanchez (Children's National Hospital), and Dr. Samantha S. Sattler, William Guo, and Jeremy Hugh (Stony Brook University Hospital).

Institutional resources from the University of Virginia Department of Radiology helped to complete this study.